

Article

# Surface Enhanced Raman Spectroscopy for In-Field Detection of Pesticides: A Test on Dimethoate Residues in Water and on Olive Leaves

Lorenzo Tognaccini <sup>1</sup>, Marilena Ricci <sup>1,2</sup> , Cristina Gellini <sup>1</sup> , Alessandro Feis <sup>1</sup> ,  
Giulietta Smulevich <sup>1,\*</sup>  and Maurizio Becucci <sup>1,2,3,\*</sup> 

<sup>1</sup> Department of Chemistry 'UgoSchiff', Università degli Studi di Firenze, via della Lastruccia 3-13, 50019 Sesto Fiorentino (Fi), Italy; lorenzo.tognaccini@unifi.it (L.T.); marilena.ricci@unifi.it (M.R.); cristina.gellini@unifi.it (C.G.); alessandro.feis@unifi.it (A.F.)

<sup>2</sup> Department of Photonics, St. Petersburg Electrotechnical University, Ul. Prof. Popova, St. Petersburg 197376, Russia

<sup>3</sup> European Laboratory for Non-Linear Spectroscopy—LENS, via N. Carrara 1, 50019 Sesto Fiorentino (Fi), Italy

\* Correspondence: giulietta.smulevich@unifi.it (G.S.); maurizio.becucci@unifi.it (M.B.)

Academic Editor: Keith C. Gordon

Received: 13 December 2018; Accepted: 10 January 2019; Published: 15 January 2019



**Abstract:** Dimethoate (DMT) is an organophosphate insecticide commonly used to protect fruit trees and in particular olive trees. Since it is highly water-soluble, its use on olive trees is considered quite safe, because it flows away in the residual water during the oil extraction process. However, its use is strictly regulated, specially on organic cultures. The organic production chain certification is not trivial, since DMT rapidly degrades to omethoate (OMT) and both disappear in about two months. Therefore, simple, sensitive, cost-effective and accurate methods for the determination of dimethoate, possibly suitable for in-field application, can be of great interest. In this work, a quick screening method, possibly useful for organic cultures certification will be presented. DMT and OMT in water and on olive leaves have been detected by surface enhanced Raman spectroscopy (SERS) using portable instrumentations. On leaves, the SERS signals were measured with a reasonably good S/N ratio, allowing us to detect DMT at a concentration up to two orders of magnitude lower than the one usually recommended for in-field treatments. Moreover, detailed information on the DMT distribution on the leaves has been obtained by Raman line- (or area-) scanning experiments.

**Keywords:** dimethoate; pesticides; SERS; olive; portable microRaman

## 1. Introduction

The balance between large-scale, cost-effective production in agriculture and the public demand of healthy food is actively pursued. Therefore, a continuous effort is made for the sustainable use of pesticides. At present, the use of pesticides is strictly regulated in many countries. Their field of application, dose and allowed residual limit are defined by public regulatory authorities and periodically revised. Different countries have specific norms concerning the allowed DMT use and dose. We will refer only to the EU regulation, however very similar rules are enforced in many other countries. Moreover, public awareness is very high and organic food is getting with time a larger and larger share of the market with a constant increase of the number of organic farms. Certification for organic food production is not trivial as some pesticides have a reduced persistence on fruits and plants. That is very good for the final quality of the products but, at the same time, it makes extremely difficult to certify the full production chain. The available analytical methods with very high sensitivity and general applicability for pesticides are mostly based on extraction and chromatographic method.

Efficient routines (QuEChERS) have been devised allowing sample cleanup and multiresidue analysis of pesticides, fully responding to the present norms [1,2]. However these methods are time consuming requiring many steps (sampling, transport to the laboratory, storage of the sample, analysis), and an advanced sample manipulation including the use of different solvents and reagents. Therefore, simple analytical methods, possibly suitable for in-field application can be of large interest. They could be used for targeted analysis of selected pesticides, thanks to the knowledge of specific problems of the different cultivars and local environmental conditions that make more likely the presence of specific pests in the field. As an example, the olive fly (*Bactrocera oleae*) is probably the most important pest affecting olives in some regions (typically the Mediterranean basin and South Africa and, more recently, California). Its presence is most relevant in areas and periods characterized by higher humidity and relatively lower temperatures. A widespread pesticide used for the olive fly control is based on dimethoate (DMT) as active substance [3]. DMT is an organophosphate insecticide and acaricide used since the '50s. It is degraded relatively rapidly following different pathways [4]. DMT, whose structure is depicted in Figure 1, is converted into its oxygenated analogous omethoate (OMT, see also Figure 1) on the leaf surfaces while the absorbed DMT is decomposed following different enzymatic reaction pathways. This is the reason for definition of regulatory limits often given as the sum of DMT and OMT content [5]. However, more recently different regulatory limits have been defined for the two pesticides [6].

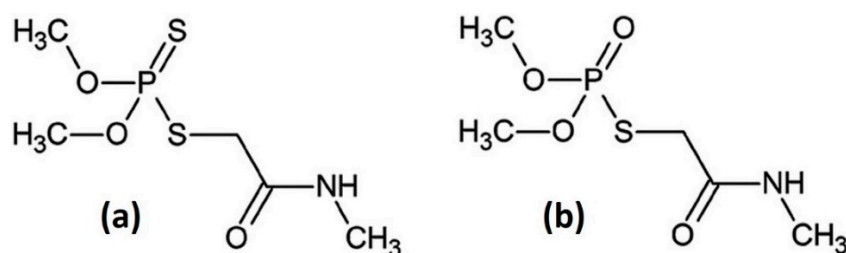


Figure 1. Schematic structures of DMT (a) and OMT (b).

DMT is suggested for treatments on olive plants as a water solution at  $10^{-2}$ – $10^{-3}$  M concentration range, according to the technical datasheet from the producer Cheminova AS for the different treatment strategies (80–625 mL of the industrial formulation containing 40% DMT in weight per 100 L of the final solution). It has a deadline deficiency (interval between treatment and use of product) of 28 days. Its persistence (either as DMT or OMT) on the surface of the olive fruit is up to 10% on the 4 weeks timescale [4,7,8]. The presence of DMT on olives for oil production is allowed to the maximum limit of 3 mg/Kg (OMT 1.5 mg/Kg) [6].

DMT is also found in water bodies following its use in field. DMT is conveniently used in the olive farms as it is highly water soluble and its transfer from olive to oil during oil production is low (about 30%) [8]. That is an interesting property for the olive oil production but poses severe issues on the treatment of the residues from olive oil production. The regulatory framework for water policies is set by international laws [9] but national limits apply for specific cases. For instance, in Italy DMT contaminated water can be sent to the sewage system if total organophosphorus pesticides concentration, which includes DMT, is below 0.1 mg/L [10]. The same limit applies for the direct discharge in surface water bodies. DMT is used not only to support olive production but also in many productions, including citrus, lettuce, tomatoes, onions, and others. Therefore, the problem is quite general and the availability of simple and effective methods for its in-field identification could be of extreme interest for the public health and for the appropriate certification of organic produce.

Recently, it has been shown that surface enhanced Raman spectroscopy (SERS) is an effective method for DMT detection both in water solution and on solid surfaces [11]. It is well known that Raman scattering intensity can increase enormously in presence of nanostructured metal surfaces, typically silver or gold [12–14]. If the molecule under investigation is efficiently adsorbed on the metal surface, it can experience an extremely high local electric field due to the nanostructured surface

topology and the resonant excitation of localized surface plasmons. Furthermore, chemical processes can affect the adsorbed molecules and modulate its polarizability, which is responsible for the scattering process itself.

In recent years, different examples of application of SERS spectroscopy for analytical purposes and more specifically for detection of pesticides on vegetables have been presented (see for instance refs. [15,16] for recent reviews). Few examples are reported in the literature for the identification of different pesticides by direct application of silver nanoparticles (AgNPs) on fruit or vegetable skin [17–25]. These experiments are carried out using confocal microscopes coupled to laboratory equipment. Very recently, this approach was used for measuring the OMT distribution on apples and peaches [26,27]. The use of portable equipment is still a challenge for identification of pesticides directly on the vegetables surface, without intermediate steps [28].

In this paper, we report new results useful for identification of olive leaves treated with DMT by means of SERS. We have determined a limit of detection for DMT in water and identified the presence of DMT on olive leaves using portable instrumentation. Therefore, this work provides a basis for in-field DMT detection in olive cultivations and on-line monitoring process for the DMT content in wastewaters from olive oil production plants.

## 2. Results and Discussion

The DMT and OMT Raman and SERS spectra have been discussed in details (including bands assignment) by Guerrini et al. [9]. The authors showed that the SERS spectra of DMT on AgNPs could not be simply related to the Raman spectrum of solid DMT, the intensity and frequency variations being much larger than usual. They suggested that AgNPs promote DMT hydrolysis to omethoate (OMT), a reaction that is known to occur also through thermal or photocatalytic mechanisms. In Figure 2 we show the comparison of the DMT (solid) Raman spectrum (Figure 2a) and the OMT SERS spectrum (Figure 2d) with SERS spectra of DMT in solution taken at different delay times after preparation.

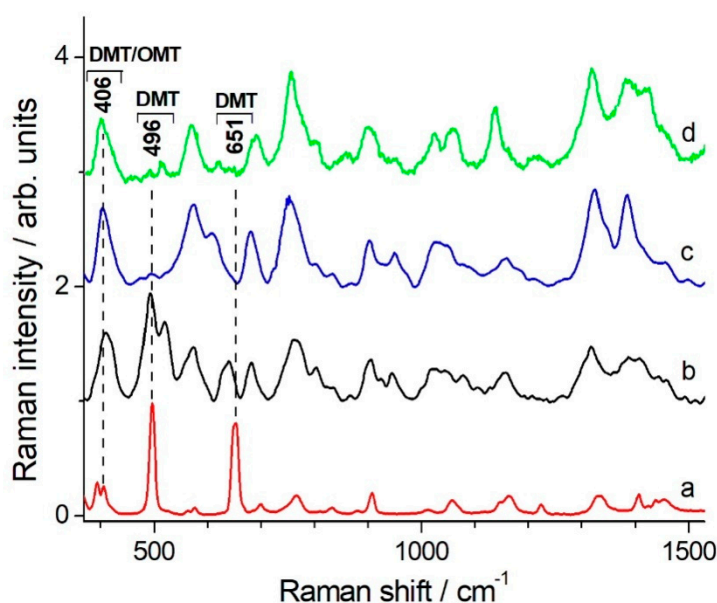


**Figure 2.** Raman spectrum of solid DMT (a), SERS spectra of  $10^{-4}$  M DMT measured immediately after sample preparation (b) or 15 min later (c), and OMT SERS spectrum (d) (adapted from Guerrini et al. [11]). Experimental details: (a) measured on microRaman Renishaw RM2000 spectrometer with 10s accumulation time and 3 averages; (b) and (c) measured on BWTek portable spectrometer with 50s accumulation time and 4 averages. Spectra are baseline corrected. The wavenumbers of the characteristic Raman bands of DMT and OMT discussed in the text are indicated.

The SERS spectrum of a freshly made solution (Figure 2b) still exhibits the strong band at  $496\text{ cm}^{-1}$  that dominates the solid DMT Raman spectrum. This band almost disappears 15 min after sample preparation and the spectrum (Figure 2c) becomes practically coincident with the OMT SERS spectrum. Therefore, these new results strongly support the hypothesis of a rapid DMT decomposition to OMT, promoted by AgNPs, in water solution.

Once the Raman/SERS spectroscopic signature of DMT was firmly established, our aim was to identify the most suitable experimental conditions for a high sensitivity DMT detection by SERS methods. Also, we have determined the limit of detection for DMT in solution under our best operative conditions and we have established a protocol for DMT identification when it is deposited and dried on solid surfaces. Our experiments have been carried with either laboratory or portable Raman setups.

AgNPs, synthesized according to the Lee-Meisel method [29], were selected as SERS active substrate. The plasmonic properties of the AgNPs were checked measuring their UV-VIS attenuation spectrum (Figure S1 in the Supplementary Information). The maximum was around 418 nm, corresponding to a most probable diameter of about 40 nm [30]. The TEM image of the AgNPs is shown in the Supplementary information, Figure S2.

SERS spectra of DMT ( $10^{-4}\text{ M}$  in the AgNPs colloidal dispersion) were obtained using excitation wavelengths at 458, 532, 633, 785, and 1064 nm. With the shorter wavelengths (458 and 532 nm), the intensity of the SERS signal was very weak (data not shown). Therefore, we worked with long-wavelength laser sources. In fact, a partial NPs aggregation induced by ions in solution caused the formation of strongly SERS-active aggregates of nanoparticles characterized by a red-shifted plasmonic band [13]. This aggregation can be followed spectroscopically by checking the changes of the UV-VIS attenuation spectrum with the concentration of these anions. Both a decrease of the peak at 418 nm and an increase of the longer wavelength wing of the signal can be clearly observed (see Supplementary Information, Figure S1). A 100 mM  $\text{KNO}_3$  concentration in solution completely destabilizes the Ag colloidal dispersion. Instead, at 40 mM  $\text{KNO}_3$  concentration the colloidal dispersion is still stable during the measurements and a strong aggregation is spectroscopically observed. As a further step, we have measured the relative SERS signal enhancement for DMT with 785 and 1064 nm excitation in the presence of 10% (*v/v*) ethanol, which is not adsorbed on AgNPs and does not destabilize the colloidal dispersion. Therefore, the strong Raman peak of ethanol at  $880\text{ cm}^{-1}$  can be used as internal standard for intensity calibration of the DMT SERS signals. As shown in Supplementary Information (Figure S3), we observed a signal enhancement approximately 2 times higher in the DMT spectrum taken with the 785 nm excitation as compared to the 1064 nm excitation. Therefore, we used the 785 nm laser excitation for the majority of the experiments. This is an advisable choice also because many portable Raman spectrometers working in this spectral range are commercially available.

The SERS analytical enhancement factor observed in our experiments with 1064 nm excitation is in the order of  $10^3$ , evaluated from the ratio of the strongest DMT bands at  $496$  and  $651\text{ cm}^{-1}$ , measured in a  $10^{-2}\text{ M}$  DMT solution in water (solubility limit) and in the SERS spectrum obtained immediately after sample preparation. This value should be taken as a lower limit for the SERS analytical enhancement factor due to the rapid DMT decomposition to OMT in the SERS samples. The DMT Raman spectrum in solution is shown in the Supplementary Information, Figure S4.

Application of SERS for quantitative analysis is quite difficult [31,32]. Also, the clear definition of the limit of detection (LOD) for an analyte in Raman/SERS spectroscopy is not straightforward. The signal-to-noise ratio depends on optical layout, characteristics of the detector, available laser power, integration time and number of averaged spectra and quality of the SERS active substrate, among the other parameters. However, for a practical application of the SERS method we must try to provide some indication: Figure 3 shows typical spectra, which were obtained with an integration time of 100 s, 5 averages, laser wavelength 785 nm, 20 mW at the sample using the portable system. The most suitable band for a quantitative data evaluation is that at  $406\text{ cm}^{-1}$ , a single peak standing out of a flat background. The peak appears to be common to DMT and OMT [11]. By the use of that reporting signal, the DMT detection limit is determined as low as  $5 \times 10^{-7}\text{ M}$ , corresponding to a

signal to noise ratio equal to 3 in the peak height determination. A good linearity for the SERS signal at  $406\text{ cm}^{-1}$  as a function of the DMT concentration was obtained in the range  $5 \times 10^{-7}$ – $1 \times 10^{-5}$  M (see Figure 4).

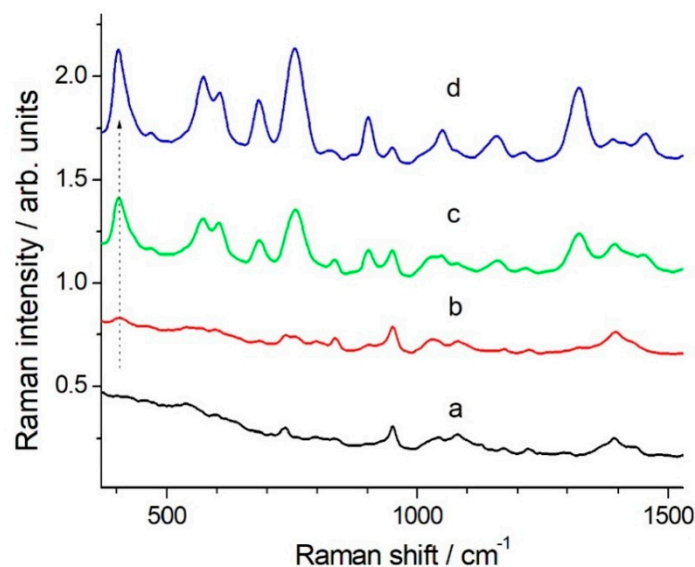


**Figure 3.** SERS spectra (785 nm excitation, BWTek portable Raman spectrometer) for different nominal DMT concentration: 0.0 (only AgNPs in water) (a),  $1 \times 10^{-6}$  (b),  $5 \times 10^{-6}$  (c),  $1 \times 10^{-5}$  M (d). Spectra are vertically shifted to improve data readability. The arrow points to the  $406\text{ cm}^{-1}$  band used for DMT quantification.

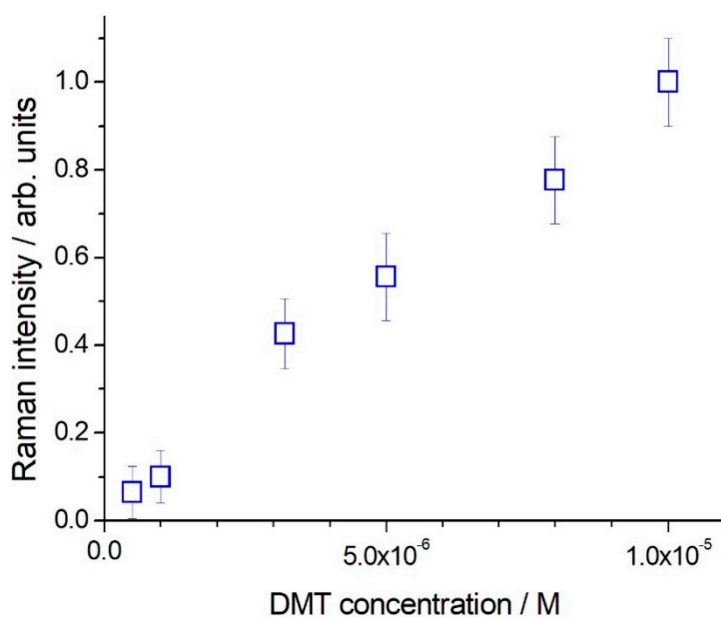


**Figure 4.** SERS signal (785 nm excitation, BWTek portable Raman spectrometer) of the band at  $406\text{ cm}^{-1}$  as a function of DMT nominal concentration, measured on three sets of samples. The standard deviation for each data point is reported.

In order to test the possibility to perform SERS experiment *in-situ* to identify DMT on olive leaves, we have measured the Raman/SERS signal originated from olive leaves obtained with the 785 nm excitation using a Raman microscope. No relevant Raman signal is originated from the bare leaf (either front or back surface), only a modest luminescence background is present. Upon deposition of AgNPs on the leaf surface, no relevant SERS signal is observed and the luminescence is slightly quenched.

As a first test carried out with laboratory equipment, we prepared mock-ups by spraying DMT and AgNPs on a glass slide and we measured their SERS spectra. In details, we sprayed on a glass slide a  $10^{-2}$  M solution of DMT with aggregated AgNPs, similar to those used for the tests in solution described above. The concentration of DMT corresponds to that recommended for in-field treatments. The sprayer produced a good aerosol that covered uniformly the surface with 20–100  $\mu\text{m}$  diameter droplets. SERS spectra with very good S/N ratio and very similar to those measured on DMT solutions (see Supplementary Information, Figure S5) have been obtained.

Furthermore, still using laboratory equipment, DMT solutions ( $10^{-2}$ – $10^{-4}$  M) were sprayed on olive leaves, later the colloidal dispersion of AgNPs was applied. We let the samples dry in air and then we measured the SERS spectra in many different points with a Raman microscope. The SERS signal was detected with a reasonably good S/N ratio even for samples spiked with DMT  $10^{-4}$  M, as shown in Figure 5a. In this case the spectrum is intermediate between that of OMT and DMT as the peak around  $500\text{ cm}^{-1}$ , characteristic of DMT, is present (or even strong and comparable to all other major features present that are typical of the OMT SERS spectrum [11]), suggesting that only a partial DMT hydrolysis has taken place on the leaf surface.

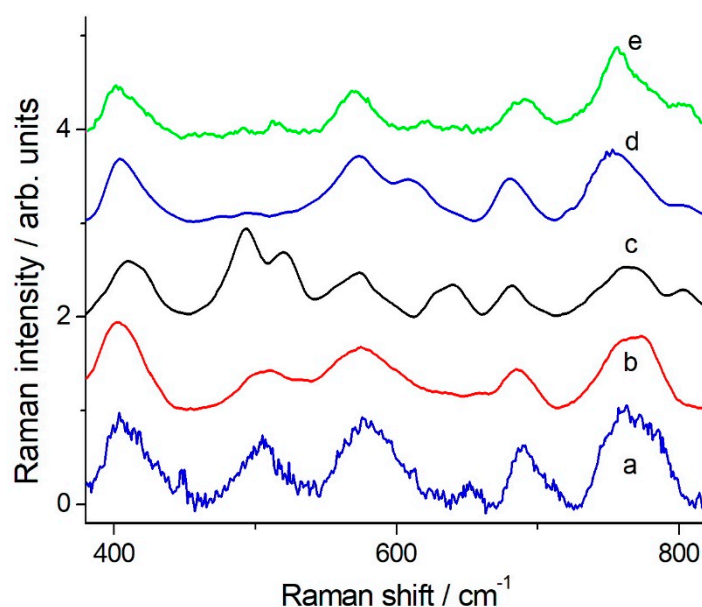


**Figure 5.** Comparison between the SERS spectra measured on olive leaves DMT spiked and SERS spectra of the standard materials in solution. (a) SERS spectrum measured with laboratory equipment on the olive leaf spiked with  $10^{-4}$  M DMT. (b) SERS spectrum measured with portable equipment on the olive leaf spiked with  $10^{-2}$  M DMT. (c) SERS spectrum of  $10^{-4}$  M DMT measured immediately after sample preparation. (d) SERS spectrum of  $10^{-4}$  M DMT measured 15 min after sample preparation. (e) OMT SERS spectrum (adapted from Guerrini et al. [11]). Experimental conditions: 785 nm laser excitation; (a) measured with Renishaw RM2000 microRaman spectrometers; (b,c,d) measured with a BWTek portable Raman spectrometer; (a) 2 mW at the sample, 20x objective, 10 s integration time, 20 averages; (b) 2.5 mW at the sample, 40x microscope objective, 10 s integration time, 10 averages; (c,d) 20 mW at the sample, macro Raman fiber probe, 50s integration time, 4 averages. All spectra are baseline corrected.

Detailed information on the DMT distribution on the leaves could be obtained by Raman line- (or area-) scanning experiments that we performed by placing the sample on a computer controlled motorized micrometric table and acquiring the spectrum in different points. As discussed above, under these experimental conditions DMT rapidly transforms to OMT. However, for the purpose of organic grown cultivation methods, what is relevant is the detection of DMT or its derivatives, not its exact quantification. Since the  $406\text{ cm}^{-1}$  Raman band does not show any major overlap with

other spectral components, only a small section of the spectrum around this band was selected for numerical elaboration (typically between 350 and 450  $\text{cm}^{-1}$ ). It was possible to fit the spectrum by using only a linear baseline and one single band with a Lorentzian profile, total five free parameters, with appropriate constrains for the band center position and bandwidth. Automatic fitting routines that operate on larger spectral regions, including many bands, do not give reliable results due to the large number of parameters needed. In Figure 6 we present the intensity signal of the 406  $\text{cm}^{-1}$  band for line-scans made across a leaf area treated with 2  $\mu\text{L}$  of AgNPs colloidal dispersion, either clean or spiked with 1  $\mu\text{L}$  of  $10^{-3}\text{M}$  DMT solution. The experiment gives virtually zero signal on the clean leaf surface or in that covered with AgNPs only. Conversely, it provides a clear signal with 10% standard error in the leaf region treated with DMT/AgNPs (visually measured as large as 3 mm). The large fluctuations of the signal intensity in the leaf spiked area are probably due to the ratio between the small sampling area accessed in each point by the confocal Renishaw Raman microscope and the scale of the sample spatial variance, that is related both to the leaf morphology and the uniformity of surface coverage with DMT/AgNPs. Images of olive leaves, clean or treated with AgNPs, are shown in the Supplementary Information (Figure S6).

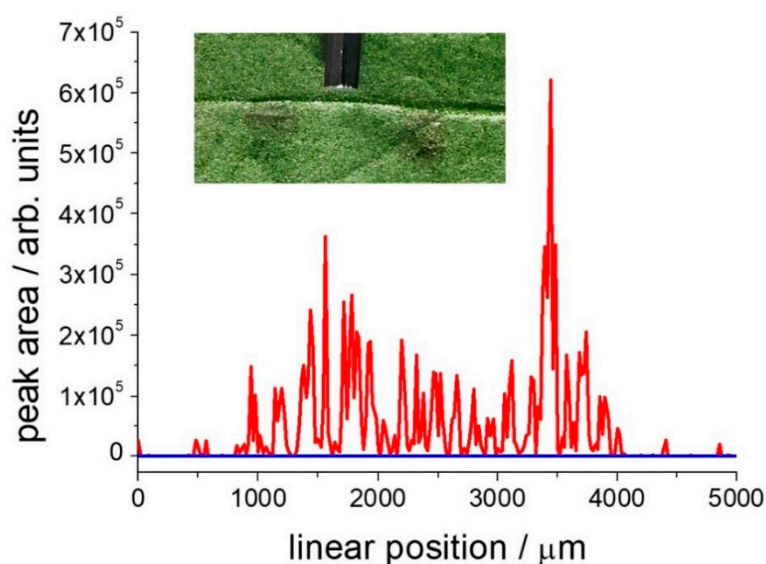


**Figure 6.** Plot of the 406  $\text{cm}^{-1}$  peak area in a 5 mm line-scan (20  $\mu\text{m}$  step) passing across a 3 mm diameter area treated with the AgNPs solution, either DMT treated or not. The flat, blue line refers to the DMT-free leaf surface; the red line refers to the DMT-treated leaf surface. The inset show a picture of the leaf and the two measured areas (DMT treated and not), possibly identified as grey circles due to the presence of AgNPs. We placed the tip of a 2 mm hex key in between the two spots to set the scale of the image. Data obtained with the Renishaw RM2000 Raman microscope.

We have also measured the SERS signal on a DMT treated olive leaf, prepared as described above, by using the portable BWTek microRaman setup. The DMT SERS spectrum on the leaf surface was obtained as the difference between the signals measured on the spiked and clean areas (the full set of data is reported in the Supplementary Information, Figure S7). The leaf area treated with DMT was spiked with 1  $\mu\text{L}$  of DMT solution  $10^{-2}\text{M}$  followed, on the dried leaf, by 2  $\mu\text{L}$  of AgNPs colloidal solution. The SERS spectrum obtained with 2.5 mW laser power showed a very good S/N ratio (Figure 5b), while a laser power above 10 mW resulted in the drop of the SERS signal and the raise of a strong background, possible indication of sample heating and desorption of the analyte from the AgNPs. The SERS spectrum measured on the leaf surface (Figure 5b) closely matches the one measured on freshly made DMT solutions (Figure 5c), suggesting the occurrence of a limited DMT hydrolysis.

Finally, we carried out a test for the detection of DMT on the olive leaves spiked with DMT water solutions at different concentration, ranging from  $10^{-2}$  to  $10^{-5}\text{M}$ , by using the portable micro-Raman

spectrometer. This measurement is representative of the in-field DMT identification at later time after treatment (it is commonly applied as a  $10^{-2}$ – $10^{-3}$  M solution and its persistence on the olive fruit surface is possibly as large as 10% after 4 weeks). Figure 7 shows the results, in a logarithmic plot, based on the average of different determinations carried out on the leaf surface DMT spiked (either with 1  $\mu$ L droplet of DMT solution or sprayed with the same solution, two replicas each) and AgNPs coated (2  $\mu$ L droplet). Our data show a good sensitivity in the  $10^{-4}$ – $10^{-2}$  M DMT concentration range, suggesting an effectiveness of the method for DMT SERS detection on leaves up to 4–8 weeks after treatment, according to the recommended treatment strategies. The non-linearity shown by the plot for high DMT contents is commonly observed in SERS quantitative applications that span a large concentration range [33]. The SERS signal depends on the interaction of the analyte with the AgNPs, a process influenced by many parameters, including the analyte concentration itself.

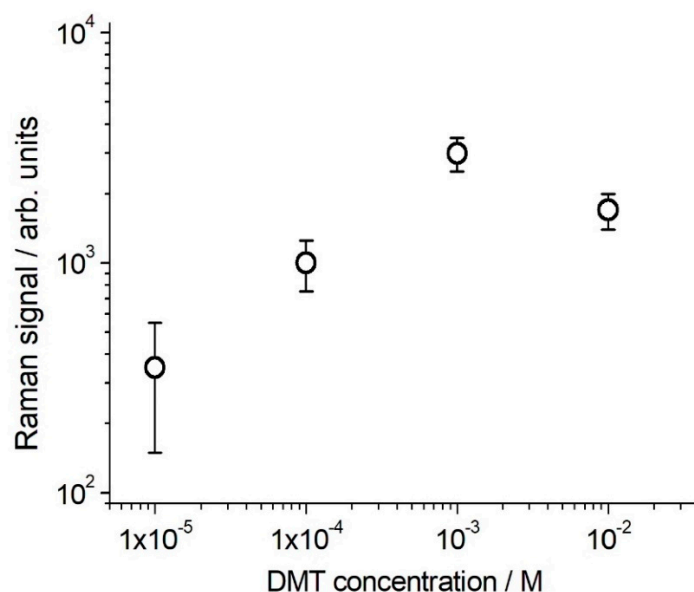


**Figure 7.** DMT determination with the BWTek portable microRaman spectrometer on olive leaves. Logarithmic plot of the SERS signal ( $406 \text{ cm}^{-1}$  band area) vs. DMT concentration. Conditions:  $40\times$  objective, 785 nm excitation wavelength, 2.5 mW laser power on the sample, 10 s integration time and 10 averages.

### 3. Materials and Methods

DMT (analytical standard quality) was purchased from Merck/Sigma-Aldrich (Darmstadt, D.) and was used without further purification. Water used for preparation of the different solutions was LC-MS chromatography grade, obtained from Merck/Sigma-Aldrich. Silver nanoparticles were prepared as colloidal dispersions according to the standard Lee-Meisel method [29]. Their extinction spectrum in the visible range was used as a probe of both dimensions distribution and aggregation [30,34].

SERS spectra in solution in standard 10 mm squared base quartz cuvette were measured in backscattering geometry either using a Bruker FT-Raman spectrometer (Bruker, Billerica, MA, USA, 1064 nm excitation, 20–300 mW on the sample) or using a portable Raman spectrometer. The latter was assembled using a 785 nm narrow-band diode laser as light source, coupled to a Raman fiber probe (InPhotonics, Norwood, MA, USA,) delivering 20 mW laser power at sample. The scattered light was fed through the fiber to an Exemplar Pro spectrometer (B&W Tek Inc., Metrohm, Herisau, Switzerland) with deep-cooled CCD detector. Solutions with concentrations ranging from  $10^{-2}$  to  $10^{-7}$  M were prepared by adding to 900  $\mu$ L of the colloidal dispersion both 40  $\mu$ L of a 1M solution of  $\text{KNO}_3$  (as aggregant) and 100  $\mu$ L of a standard DMT solution in water. SERS spectra were measured almost immediately after sample preparation. Preliminary tests for assessment of the best excitation wavelength were made also on a table-top Raman spectrometer consisting of a SP150 monochromator

(Acton Optics, Acton, MA, USA) with a Pixis CCD detector (Princeton Instruments, Trenton, NJ, USA) and excitation laser sources at 457, 532 and 632 nm). Due to the spectral dependence of the SERS enhancement factor on the excitation wavelength, significant SERS spectra were obtained only for long wavelength excitation and the data in the Results section refer to these experimental conditions. For a more refined evaluation of the SERS enhancement factor ratio between 785 and 1064 nm excitation, the SERS measurements were repeated adding ethanol as internal standard (10% in volume).

SERS spectra on DMT solutions dried on surfaces (glass slide or olive leaves) were measured on samples prepared by using two different procedures. In the first, the samples described above ( $10^{-2}$ – $10^{-4}$  M DMT solutions in presence of AgNPs) were sprayed on the glass/leaves surface. In the second, more realistic samples were prepared by deposition of 1  $\mu$ L of  $10^{-2}$  M DMT water solution followed, after 1 h, by deposition on the same spot of 2  $\mu$ L drop of colloidal dispersion aggregated by  $\text{KNO}_3$  (see above). Laboratory measurements were carried out on a RM2000 Raman microscope (Renishaw, Wotton-under-Edge, UK) equipped with a 20 $\times$  microscope objective, on a 3  $\mu$ m diameter spot. Raman mapping was performed by moving the sample on a motorized micrometric table, acquiring the spectrum in different points and plotting the intensity of a representative band as a function of the sampling point position. In order to assess feasibility of in-field measurements, final tests were performed, still in laboratory, by using a portable microscope assembly built using BWTek spectrometer with the BAC151B micro-sampling system. It allows to obtain with the 40 $\times$  microscope objective a laser spot about 50  $\mu$ m diameter in the focal plane, much larger than the Renishaw laboratory Raman microscope.

#### 4. Conclusions

The application of SERS for in-field detection of olive cultures treated with DMT allows us to reach a good level of sensitivity by direct measurements on olive leaves. Given the usual initial treatment dose and a DMT decay rate of about 90% in 4 weeks, DMT treatment could be detected up to 1–2 months after its use. The period of DMT application in-field can be predicted with reasonable accuracy given the local weather and the spread of the pest in the local area. Therefore, this method can be useful to assess the effective DMT use in field, at least at the level of pre-screening tests.

The DMT detection in water samples could be obtained quantitatively, thanks to a good calibration or the use of the well-known Standard Addition Method. We observed a linear dependence of the SERS signal of DMT in the range  $5 \times 10^{-7}$ – $1 \times 10^{-5}$  M. This sensitivity could be useful for monitoring waste water in olive oil production sites.

**Supplementary Materials:** The following are available online at <http://www.mdpi.com/1420-3049/24/2/292/s1>, Figure S1: The attenuation spectrum (2 mm path-length) of the colloidal dispersion with AgNPs from synthesis and with different concentration of  $\text{KNO}_3$  (aggregant), Figure S2: TEM image of partly aggregated AgNPs deposited on a clean surface, Figure S3: Raman spectrum of ethanol taken with the 785 nm excitation (a), and SERS spectra of  $10^{-4}$  M DMT taken with the 1064 (b) and 785 nm (c) excitation, in presence of 10% ethanol. The arrow points to the ethanol strong band ( $880 \text{ cm}^{-1}$ ) used to evaluate the relative SERS enhancement factors. Spectra are baseline corrected, Figure S4: Raman spectrum of DMT  $10^{-2}$  M in water (Bruker FT-Raman spectrometer, 1064 nm, 300 mW, 5000 averages, background subtracted), Figure S5: Comparison of solid DMT Raman spectrum (a) with SERS spectra of  $10^{-4}$  M DMT (b) and of the same solution sprayed on a glass surface and dried (c). (a) and (c) measured on microRaman Renishaw RM2000 spectrometer; (b) measured on BWTek portable spectrometer, Figure S6: Microscope bright field images of clean and AgNPs treated olive leaves. (a), (b) clean olive leaf (back side) observed with 10x and 100x objectives, reflection mode; (c) clean leaf (back side), 100x objective, transmission mode; (d) olive leaf treated on the back side with aggregated AgNPs, 100x objective, transmission mode; Figure S7: Measurements with the BWTek portable micro-Raman spectrometer: (a) SERS spectrum of the DMT treated area of an olive leaf ( $10^{-2}$  M DMT), (b) Raman spectrum of the clean leaf, and (c) their difference spectrum. Experimental details: 40 $\times$  objective, 785 nm excitation wavelength, 2.5 mW laser power on the sample, 10 s integration time and 10 averages. The inset shows the difference spectrum (background subtracted) that in Figure 5 is compared to those obtained from DMT/OMT solutions.

**Author Contributions:** Conceptualization, G.S. and M.B.; Formal analysis, L.T., C.G., A.F., G.S. and M.B.; Funding acquisition, M.B.; Investigation, L.T., A.F. and M.B.; Methodology, M.R.; Project administration, G.S. and M.B.; Supervision, A.F., G.S. and M.B.; Writing—original draft, G.S. and M.B.; Writing—review & editing, L.T., M.R., C.G., A.F., G.S. and M.B.

**Funding:** This work was supported by the EnteCassa di Risparmio di Firenze (grant n. 2016/13363), the E.U. (Laserlab-Europe, H2020 EC-GA 654148) and the University of Florence.

**Acknowledgments:** The Authors wish to thank C. Bruni (CDR S.r.l., Italy), M. Nocentini (IZSLT, Italy) and D. Santianni (Publiacqua S.p.A., Italy) for helpful discussions and suggestions.

**Conflicts of Interest:** The authors declare that there are no conflicts of interest.

## Abbreviations

AgNPs	Silver nanoparticles
CCD	Charge coupled device
DMT	Dimethoate
LOD	Limit of detection
OMT	Omethoate
SERS	Surface Enhanced Raman Spectroscopy
S/N	Signal to noise
TEM	Transmission electron microscopy

## References

1. Brondi, S.H.G.; de Macedo, A.N.; Vicente, G.H.L.; Nogueira, A.R.A. Evaluation of the QuEChERS method and gas chromatography-mass spectrometry for the analysis pesticide residues in water and sediment. *Bull. Environ. Contam. Toxicol.* **2011**, *86*, 18–22. [[CrossRef](#)] [[PubMed](#)]
2. Lehotay, S.J.; Son, K.A.; Kwon, H.; Koesukwiwat, U.; Fu, W.; Mastovska, K.; Hoh, E.; Leepipatpiboon, N. Comparison of QuEChERS sample preparation methods for the analysis of pesticide residues in fruits and vegetables. *J. Chromatogr. A* **2010**, *1217*, 2548–2560. [[CrossRef](#)] [[PubMed](#)]
3. European Council Regulation (EC) No 1107/2009 of the European Parliament and of the Council of 21 October 2009 concerning the placing of plant protection products on the market and repealing Council Directives 79/117/EEC and 91/414/EEC. *Off. J. Eur. Commun.* **2009**, *52*, 1–50.
4. Dauterman, W.C.; Viado, G.B.; Casida, J.E.; O'Brien, R.D. Insecticide Residues, Persistence of Dimethoate and Metabolites Following Foliar Application to Plants. *J. Agric. Food Chem.* **1960**, *8*, 115–119. [[CrossRef](#)]
5. European Council Regulation (EC) No 396/2005 of the European Parliament and of the Council of 23 February 2005 on maximum residue levels of pesticides in or on food and feed of plant and animal origin and amending Council Directive 91/414/EEC with EEA relevance. *Off. J. Eur. Union* **2005**, *48*, 1–16.
6. European Council Commission Regulation (EU) 2017/1135 of 23 June 2017 amending Annexes II and III to Regulation (EC) No 396/2005 of the European Parliament and of the Council as regards maximum residue levels for dimethoate and omethoate in or on certain products. *Off. J. Eur. Union* **2017**, *60*, 28–51.
7. Ferreira, J.R.; Tainha, A.M. Organophosphorous insecticide residues in olives and olive oil. *Pestic. Sci.* **1983**, *14*, 167–172. [[CrossRef](#)]
8. Cabras, P.; Angioni, A.; Garau, V.L.; Melis, M.; Pirisi, F.M.; Karim, M.; Minelli, E.V. Persistence of Insecticide Residues in Olives and Olive Oil. *J. Agric. Food Chem.* **1997**, *45*, 2244–2247. [[CrossRef](#)]
9. European Council Directive 2000/60/EC of the European Parliament and of the Council of 23 October 2000 establishing a framework for Community action in the field of water policy. *Off. J. Eur. Commun.* **2000**, *43*, L327/1–L327/72.
10. Decreto legislativo recante disposizioni sulla tutela delle acque dall'inquinamento e recepimento della direttiva 91/271/Cee concernente il trattamento delle acque reflue urbane e della direttiva 91/676/Cee relativa alla protezione delle acque dall'inquin. *Gazz. Uff. Della Repubbl. Ital.* **1999**, *124*.
11. Guerrini, L.; Sanchez-Cortes, S.; Cruz, V.L.; Martinez, S.; Ristori, S.; Feis, A. Surface-enhanced Raman spectra of dimethoate and omethoate. *J. Raman Spectrosc.* **2011**, *42*, 980–985. [[CrossRef](#)]
12. Aroca, R. *Surface-Enhanced Vibrational Spectroscopy*; John Wiley & Sons, Ltd.: Chichester, UK, 2006; ISBN 9780470035641.
13. Le Ru, E.C.; Etchegoin, P.G. *Principles of Surface-Enhanced Raman Spectroscopy*; Elsevier: Amsterdam, The Netherlands, 2009; ISBN 978-0-444-52779-0.
14. Schlücker, S. *Surface Enhanced Raman Spectroscopy*; Wiley-VCH: Weinheim, Germany, 2010; ISBN 9783527632756.

15. Cialla, D.; März, A.; Böhme, R.; Theil, F.; Weber, K.; Schmitt, M.; Popp, J. Surface-enhanced Raman spectroscopy (SERS): Progress and trends. *Anal. Bioanal. Chem.* **2012**, *403*, 27–54. [[CrossRef](#)] [[PubMed](#)]
16. Pang, S.; Yang, T.; He, L. Review of surface enhanced Raman spectroscopic (SERS) detection of synthetic chemical pesticides. *TrAC Trends Anal. Chem.* **2016**, *85*, 73–82. [[CrossRef](#)]
17. Di Anibal, C.V.; Marsal, L.F.; Callao, M.P.; Ruisánchez, I. Surface Enhanced Raman Spectroscopy (SERS) and multivariate analysis as a screening tool for detecting Sudan I dye in culinary spices. *Spectrochim. Acta Part A Mol. Biomol. Spectrosc.* **2012**, *87*, 135–141. [[CrossRef](#)] [[PubMed](#)]
18. Liu, B.; Han, G.; Zhang, Z.; Liu, R.; Jiang, C.; Wang, S.; Han, M.-Y. Shell Thickness-Dependent Raman Enhancement for Rapid Identification and Detection of Pesticide Residues at Fruit Peels. *Anal. Chem.* **2012**, *84*, 255–261. [[CrossRef](#)] [[PubMed](#)]
19. Li, X.; Zhang, S.; Yu, Z.; Yang, T. Surface-Enhanced Raman Spectroscopic Analysis of Phorate and Fenthion Pesticide in Apple Skin Using Silver Nanoparticles. *Appl. Spectrosc.* **2014**, *68*, 483–487. [[CrossRef](#)] [[PubMed](#)]
20. Gong, Z.; Wang, C.; Wang, C.; Tang, C.; Cheng, F.; Du, H.; Fan, M.; Brolo, A.G. A silver nanoparticle embedded hydrogel as a substrate for surface contamination analysis by surface-enhanced Raman scattering. *Analyst* **2014**, *139*, 5283–5289. [[CrossRef](#)] [[PubMed](#)]
21. Fan, Y.; Lai, K.; Rasco, B.A.; Huang, Y. Analyses of phosmet residues in apples with surface-enhanced Raman spectroscopy. *Food Control* **2014**, *37*, 153–157. [[CrossRef](#)]
22. Fan, Y.; Lai, K.; Rasco, B.A.; Huang, Y. Determination of carbaryl pesticide in Fuji apples using surface-enhanced Raman spectroscopy coupled with multivariate analysis. *LWT Food Sci. Technol.* **2015**, *60*, 352–357. [[CrossRef](#)]
23. Tang, X.; Dong, R.; Yang, L.; Liu, J. Fabrication of Au nanorod-coated Fe<sub>3</sub>O<sub>4</sub> microspheres as SERS substrate for pesticide analysis by near-infrared excitation. *J. Raman Spectrosc.* **2015**, *46*, 470–475. [[CrossRef](#)]
24. Li, J.-L.; Sun, D.-W.; Pu, H.; Jayas, D.S. Determination of trace thiophanate-methyl and its metabolite carbendazim with teratogenic risk in red bell pepper (*Capsicum annuum* L.) by surface-enhanced Raman imaging technique. *Food Chem.* **2017**, *218*, 543–552. [[CrossRef](#)] [[PubMed](#)]
25. Wang, K.; Huang, M.; Chen, J.; Lin, L.; Kong, L.; Liu, X.; Wang, H.; Lin, M. A “drop-wipe-test” SERS method for rapid detection of pesticide residues in fruits. *J. Raman Spectrosc.* **2018**, *49*, 493–498. [[CrossRef](#)]
26. Chen, J.; Dong, D.; Ye, S. Detection of pesticide residue distribution on fruit surfaces using surface-enhanced Raman spectroscopy imaging. *RSC Adv.* **2018**, *8*, 4726–4730. [[CrossRef](#)]
27. Yaseen, T.; Sun, D.-W.; Pu, H.; Pan, T.-T. Detection of Omethoate Residues in Peach with Surface-Enhanced Raman Spectroscopy. *Food Anal. Methods* **2018**, *11*, 2518–2527. [[CrossRef](#)]
28. Pilot, R. SERS detection of food contaminants by means of portable Raman instruments. *J. Raman Spectrosc.* **2018**, *49*, 954–981. [[CrossRef](#)]
29. Lee, P.C.; Meisel, D. Adsorption and surface-enhanced Raman of dyes on silver and gold sols. *J. Phys. Chem.* **1982**, *86*, 3391–3395. [[CrossRef](#)]
30. Steingeweg, D.; Schlücker, S. Monodispersity and size control in the synthesis of 20–100 nm quasi-spherical silver nanoparticles by citrate and ascorbic acid reduction in glycerol–water mixtures. *Chem. Commun.* **2012**, *48*, 8682. [[CrossRef](#)]
31. Bell, S.E.J.; Sirimuthu, N.M.S. Quantitative surface-enhanced Raman spectroscopy. *Chem. Soc. Rev.* **2008**, *37*, 1012. [[CrossRef](#)] [[PubMed](#)]
32. Goodacre, R.; Graham, D.; Faulds, K. Recent developments in quantitative SERS: Moving towards absolute quantification. *TrAC Trends Anal. Chem.* **2018**, *102*, 359–368. [[CrossRef](#)]
33. Ricci, M.; Trombetta, E.; Castellucci, E.; Becucci, M. On the SERS quantitative determination of organic dyes. *J. Raman Spectrosc.* **2018**, *49*, 997–1005. [[CrossRef](#)]
34. Pillai, Z.S.; Kamat, P.V. What Factors Control the Size and Shape of Silver Nanoparticles in the Citrate Ion Reduction Method? *J. Phys. Chem. B* **2003**, *108*, 945–951. [[CrossRef](#)]

**Sample Availability:** Samples of the compounds are available from the authors.



© 2019 by the authors. Licensee MDPI, Basel, Switzerland. This article is an open access article distributed under the terms and conditions of the Creative Commons Attribution (CC BY) license (<http://creativecommons.org/licenses/by/4.0/>).